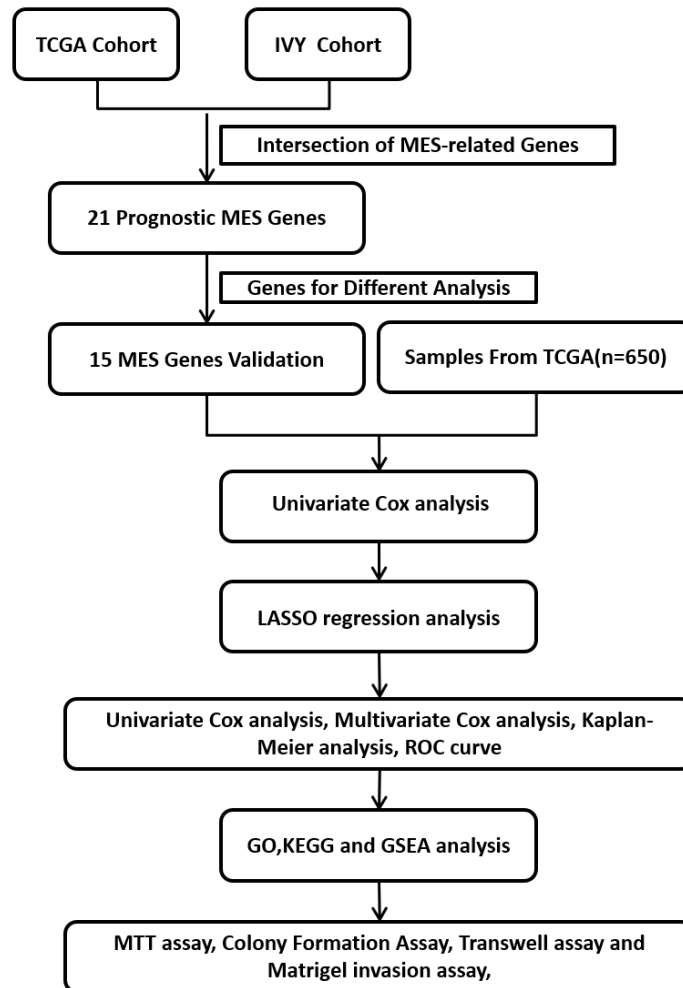
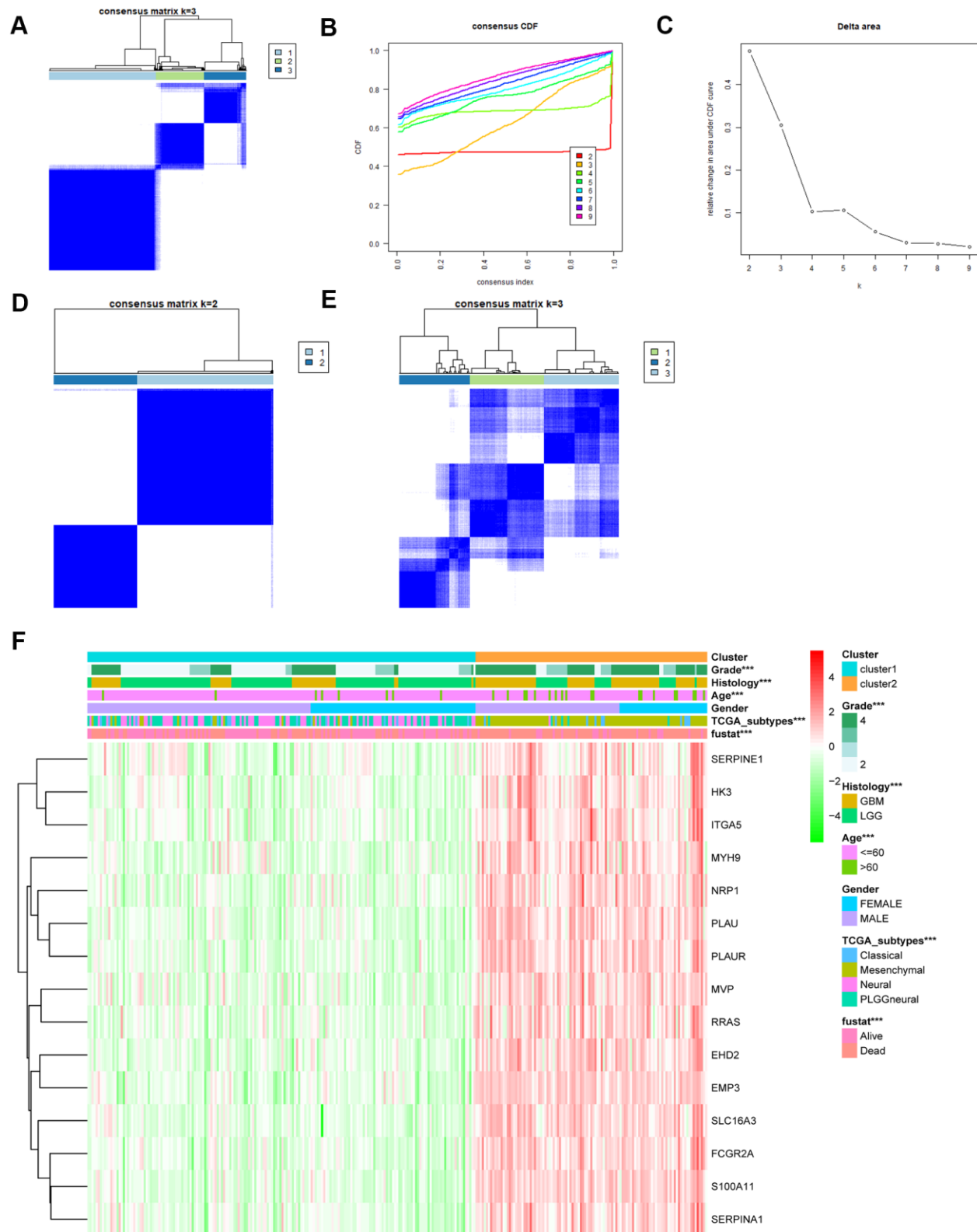


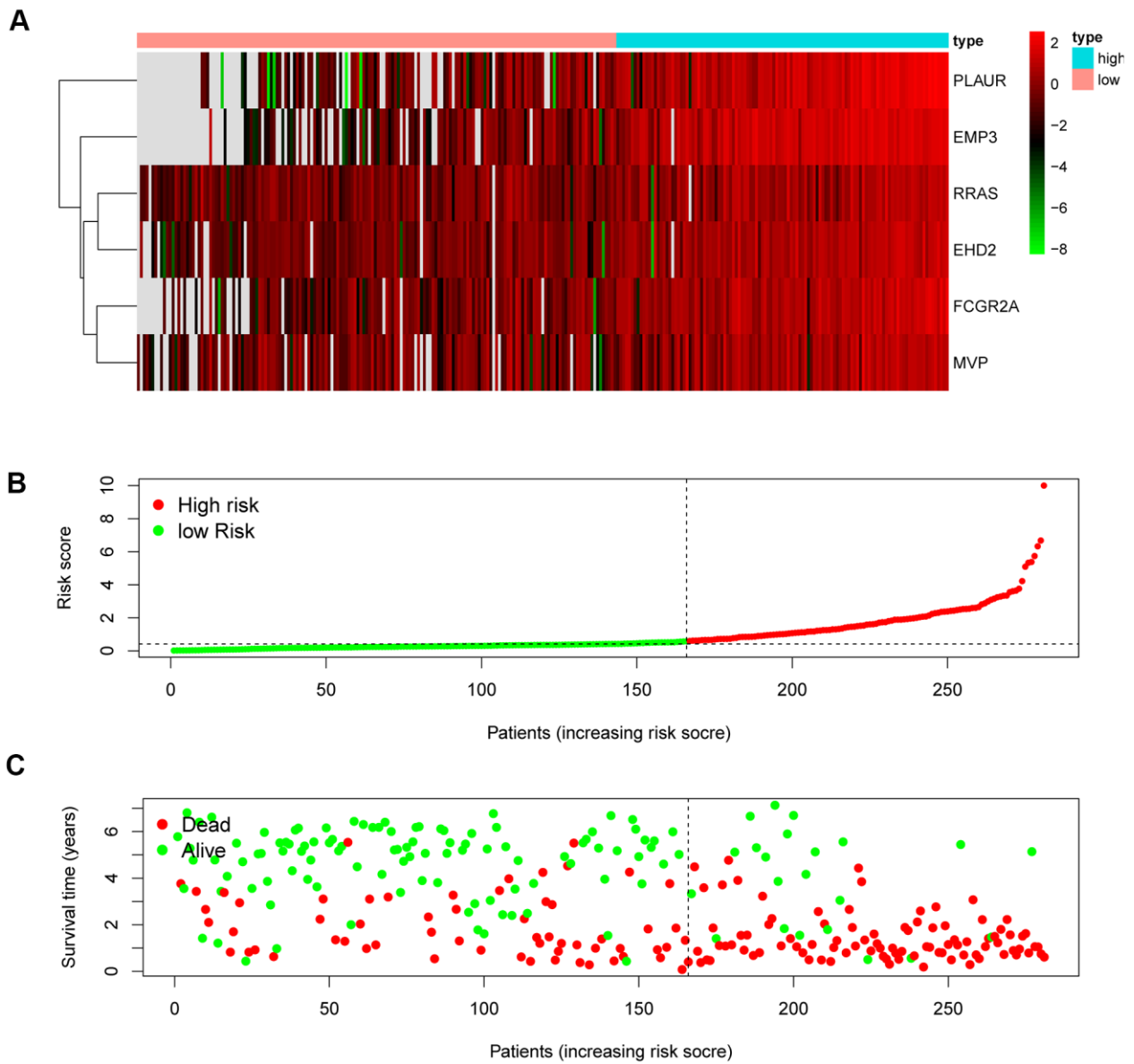
## SUPPLEMENTARY FIGURES



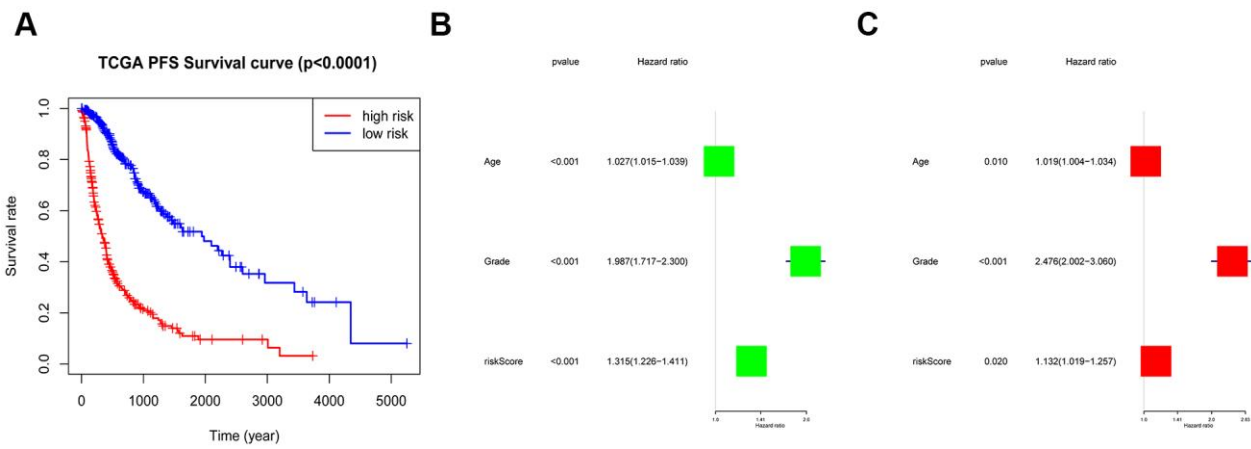
Supplementary Figure 1. The workflow of this study: data collection, analysis, and validation.



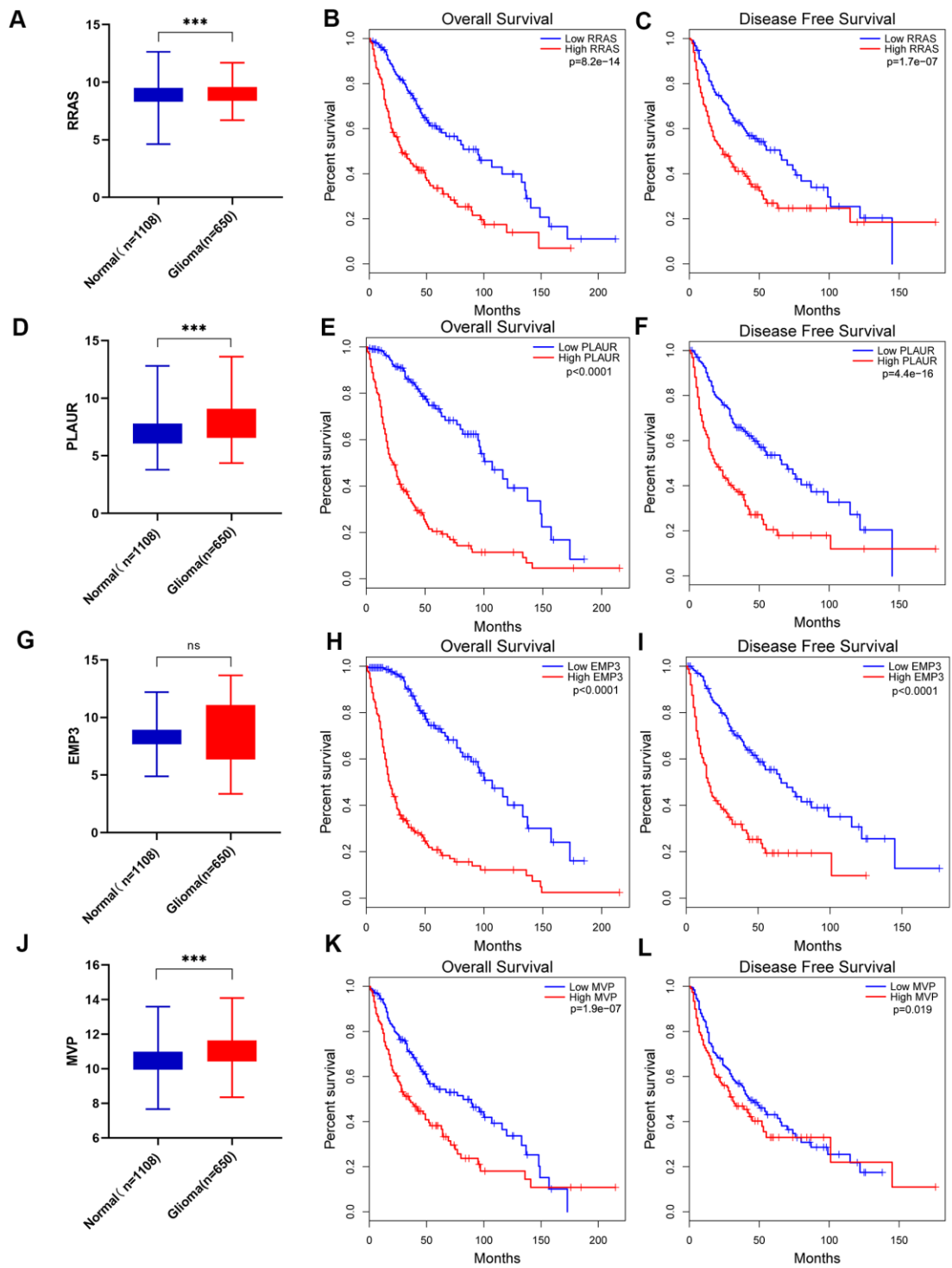
**Supplementary Figure 2. Stratification and verification of glioma based on 15 MES-related genes in the CGGA cohort.** (A) Consensus clustering matrix of 650 TCGA samples for  $k = 3$ . (B) Relative change in the area under the CDF curve for  $k = 2$  to  $k = 9$  in the testing set. (C) Consensus clustering CDF for  $k = 2$  to  $k = 9$  in the testing set. (D, E) Consensus clustering matrix of 280 CGGA samples for  $k = 2$  and  $k = 3$ . (F) Heat map of MES-related genes between CGGA cluster 1 and cluster 2 used to verify consensus clustering based on TCGA. CDF, cumulative distribution function; \*\* $P < 0.01$ ; \*\*\* $P < 0.001$ .



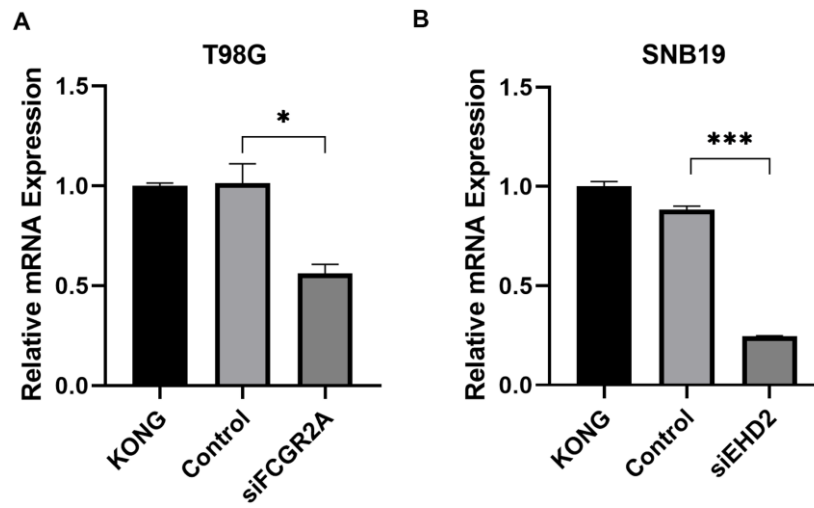
**Supplementary Figure 3. Verification of the 6-gene risk signature in CGGA datasets.** (A) Heat map shows the expression difference of six MES-related genes between the high-risk group and the low-risk group. (B) Risk curve represents the risk score and distribution of 280 cases from the CGGA database. (C) The survival status graph shows the difference in survival time of 280 cases from the CGGA database (each point represents a sample, B, C).



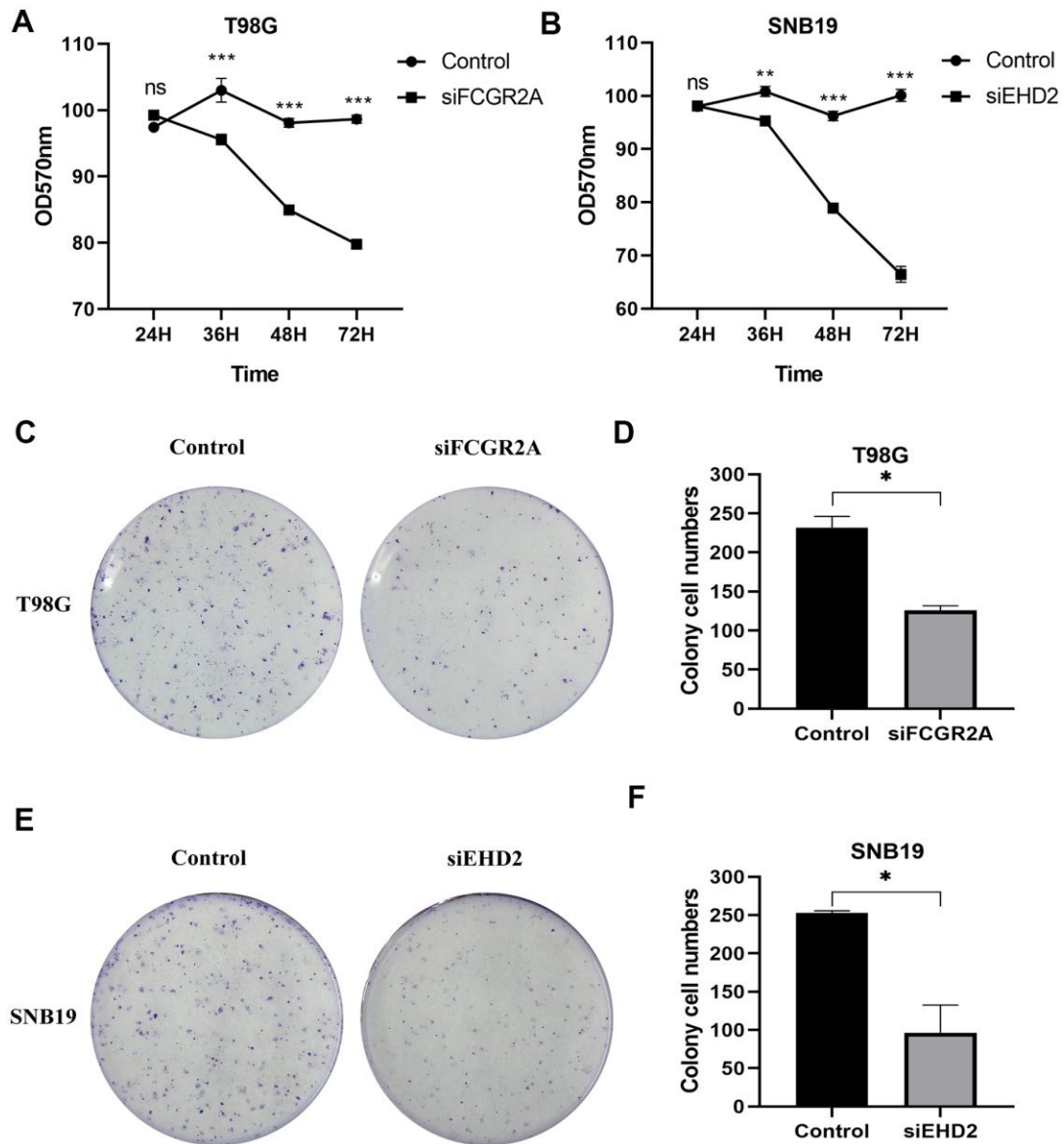
**Supplementary Figure 4. CGGA confirms the independent prognostic value of the risk score.** (A) Progression-free survival analysis between the high- and low-risk groups in the TCGA cohort. (B) Univariate Cox regression analysis of clinical pathologic features for OS in the CGGA cohort. (C) Multivariate Cox regression analysis of clinical pathologic features for OS in the CGGA cohort.



**Supplementary Figure 5. RRAS, PLAUR, EMP3 and MVP gene expression differences and survival rate differences.** (A) Differences in RRAS expression between the normal group and the glioma group from the TCGA and GTEX data. (B, C) Overall survival analysis (B) and disease-free survival analysis (C) of the relationship between RRAS expression level and survival time from the TCGA database. (D) Differences in PLAUR expression between the normal group and the glioma group from the TCGA and GTEX data. (E, F) Overall survival analysis (E) and disease-free survival analysis (F) of the relationship between PLAUR expression level and survival time from the TCGA database. (G) Differences in EMP3 expression between the normal group and the glioma group from the TCGA and GTEX data. (H, I) Overall survival analysis (H) and disease-free survival analysis (I) of the relationship between EMP3 expression level and survival time from the TCGA database. (J) Differences in MVP expression between the normal group and the glioma group from the TCGA and GTEX data. (K, L) Overall survival analysis (K) and disease-free survival analysis (L) of the relationship between MVP expression level and survival time from the TCGA database. Ns: no significance; \*\*\*p<0.001.



**Supplementary Figure 6.** The effect of FCGR2A being silenced by siFCGR2A (pro) in T98G (A) and the effect of EHD2 being silenced by siEHD2 (2) in SNB19 (B). KONG stands for untreated cell; Control stands for Negative control group. \* $P < 0.05$ ; \*\*\* $P < 0.001$ .



**Supplementary Figure 7. The effect of glioma cell clone and proliferation ability after silencing FCGR2A or EHD2.** (A, B) Cell proliferation was measured by MTT assay for 24 hours up to 72 hours. (C, D) Representative imaging (C) or counting (D) of the colonies formed by T98G cells after silencing with FCGR2A for 9 days. (E, F) Representative imaging (E) or counting (F) of the colonies formed by SNB19 cells after silencing with EHD2 for 7 days. Ns: no significance; \*P<0.05; \*\*P<0.01; \*\*\*P<0.001.